WATERSHED FROM PROPAGATED MARKERS IMPROVED BY THE COMBINATION OF SPATIO-TEMPORAL GRADIENT AND BINDING OF MARKERS HEURISTICS

Franklin César Flores
Department od Informatics, State University of Maringá
Av. Colombo, 5790 - Zona 7, Maringá, Brazil

Roberto de Alencar Lotufo
School of Electrical and Computing Engineering, University of Campinas
PO Box 6101, Campinas, Brazil

Keywords: Object segmentation in image sequences, Watershed from propagated markers, Temporal gradient.

Abstract: This paper presents the improvement of the watershed from propagated markers, a generic method to interactive segmentation of objects in image sequences, by the inclusion of a temporal gradient to the segmentation framework. Segmentation is done by applying the watershed from markers to a gradient image extracted from the temporal gradient sequence and using markers provided by the binding of markers heuristics. The performance of the improved method is demonstrated by application of a benchmark that supports a quantitative evaluation of assisted segmentation of objects in image sequences. Experimental results provided by the combination of temporal gradient with the binding of markers heuristics show that the proposed improvement can decrease the number of human interferences and the time required to process the sequences.

1 INTRODUCTION

The assisted segmentation of objects in image sequences by application of an extension of the watershed transform to the 3-D case appears to be a good solution to this kind of problem. The watershed definition is extensible to the 3-D case by applying it to a spatio-temporal gradient computed considering the image deck as an image volume and using a 3-D structuring element. With well placed markers, the 3-D segmentation may provide very good results.

However, its application is not viable for interactive segmentation, for several reasons. First, the 3-D watershed application is very time consuming: the greater the image sequence, the longer the 3-D watershed takes to segment all sequence. More, it is even worst if this segmentation process needs to be achieved every time the user makes an interference. Second, despite the good results 3-D watershed may provide, it is also the source of a kind of interframe error segmentation: the 3-D segmentation of an object may flow back and forth in the sequence to regions that does not represent the object in other instant times. Third, this process is not a progressive edition: every time a user makes an interference, the segmentation in the sequence needs to be whole inspected.

It could be interesting to exploit the good side of the 3-D assisted morphologic segmentation presented above avoiding those side effects. The idea is to include the spatio-temporal gradient, that holds spatio-temporal information from the image sequence, to the *watershed from propagated markers*, a generic method to interactive segmentation of objects in image sequences (F. C. Flores and R. A. Lotufo, 2009; Flores and Lotufo, 2003). This method consists in a combination of the watershed from markers (Beucher and Meyer, 1992; Soille and Vincent, 1990) with motion estimation techniques (S. S. Beauchemin and J. L. Barron, 1995; J. L. Barron; D. J. Fleet and S. S. Beauchemin, 1994). The segmentation technique is tied to the motion estimation one, since the markers to the objects of interest are propagated to the next frames in order to track such objects.

Flores F. and de Alencar Lotufo R. (2010).
WATERSHED FROM PROPAGATED MARKERS IMPROVED BY THE COMBINATION OF SPATIO-TEMPORAL GRADIENT AND BINDING OF MARKERS HEURISTICS.
In *Proceedings of the International Conference on Computer Vision Theory and Applications*, pages 164-172
DOI: 10.5220/0002827201640172
Copyright © SciTePress

The *binding of markers* (F. C. Flores and R. A. Lotufo, 2007) is an improvement to the watershed from propagated markers. It consists in to compute pairs of markers along the border, and each pair is composed by an internal marker and an external one. Both markers in the pair must be propagated by the same displacement vector, and this vector is computed by the motion estimation of the area *between* the pair of markers. This heuristics provides more information to the motion estimation and helps the motion of the pair of markers to follow the motion of the border that crosses the region between them in the previous frame.

This paper introduces the combination of spatio-temporal gradient with the binding of markers heuristics, in the watershed from propagated markers context. The segmentation of a given frame is done by applying the watershed from markers to a gradient extracted from a spatio-temporal gradient sequence and using markers provided by the binding of markers heuristics.

Experiments were done in order to demonstrate the performance of such combination. The demonstration was done by application of a benchmark that supports a quantitative evaluation of assisted segmentation of objects in image sequences (F. C. Flores and R. A. Lotufo, 2008). The benchmark application showed a significant decrease in the number of interferences and a increase in the segmentation results.

The paper is organized as follows: Section 2 presents some preliminary concepts. Section 3 reviews the watershed from propagated markers framework and the binding of markers heuristics and presents the spatio-temporal gradient added to the segmentation framework. Section 4 shows and discusses some experimental results and, finally, Section 5 concludes the paper with a brief discussion.

2 PRELIMINARY REVIEW

Let us define some sets used in the formalizations introduced along the paper. Let $E = \mathbb{Z} \times \mathbb{Z}$ be an *image domain*. Let $F = E \times \{1, 2, \ldots, n\}$ be the *sequence domain*, where $n \in \mathbb{Z}_+$. Let $E = F$, when $n = 1$. Let $K = [0, k]$ be a totally ordered set and let $C = K \times K \times K$.

Let $Fun[E,K]$ be the set of all functions $gs : E \rightarrow K$, denoting the set of all *grayscale images*. Let $Fun[E,C]$ be the set of all functions $cs : E \rightarrow C$, that denotes the set of all *color* (or *multiband*) *images*. Let $Fun[F,K]$ be the set of all *grayscale sequences* and let $Fun[F,C]$ be the set of all *color sequences*.

Let $i \in \{1, 2, \ldots, n\}$. Let $gs \in Fun[F,K]$ and $cs \in Fun[F,C]$. The set of all $gs(x,i)$, $\forall x \in E$ denotes the i-th *frame* of the grayscale sequence *gs*. The set of all $cs(x,i)$ denotes the i-th frame of the multiband sequence *cs*, $\forall x \in E$.

2.1 3-D Structuring Elements

Let us define the 3-D structuring elements (s.e.) that defines the 3-D connectivity in this paper:

$$B_5 = \left[\begin{pmatrix} \cdot & \cdot & \cdot \\ \cdot & \cdot & \cdot \\ \cdot & \cdot & \cdot \end{pmatrix}, \begin{pmatrix} \cdot & \bullet & \cdot \\ \bullet & \underline{\bullet} & \bullet \\ \cdot & \bullet & \cdot \end{pmatrix}, \begin{pmatrix} \cdot & \cdot & \cdot \\ \cdot & \bullet & \cdot \\ \cdot & \cdot & \cdot \end{pmatrix} \right]$$

$$B_6 = \left[\begin{pmatrix} \cdot & \cdot & \cdot \\ \cdot & \bullet & \cdot \\ \cdot & \cdot & \cdot \end{pmatrix}, \begin{pmatrix} \cdot & \bullet & \cdot \\ \bullet & \underline{\bullet} & \bullet \\ \cdot & \bullet & \cdot \end{pmatrix}, \begin{pmatrix} \cdot & \cdot & \cdot \\ \cdot & \bullet & \cdot \\ \cdot & \cdot & \cdot \end{pmatrix} \right]$$

$$B_{17} = \left[\begin{pmatrix} \cdot & \cdot & \cdot \\ \cdot & \cdot & \cdot \\ \cdot & \cdot & \cdot \end{pmatrix}, \begin{pmatrix} \bullet & \bullet & \bullet \\ \bullet & \underline{\bullet} & \bullet \\ \bullet & \bullet & \bullet \end{pmatrix}, \begin{pmatrix} \bullet & \bullet & \bullet \\ \bullet & \bullet & \bullet \\ \bullet & \bullet & \bullet \end{pmatrix} \right]$$

$$B_{26} = \left[\begin{pmatrix} \bullet & \bullet & \bullet \\ \bullet & \bullet & \bullet \\ \bullet & \bullet & \bullet \end{pmatrix}, \begin{pmatrix} \bullet & \bullet & \bullet \\ \bullet & \underline{\bullet} & \bullet \\ \bullet & \bullet & \bullet \end{pmatrix}, \begin{pmatrix} \bullet & \bullet & \bullet \\ \bullet & \bullet & \bullet \\ \bullet & \bullet & \bullet \end{pmatrix} \right]$$

Each s.e. is denoted by three 3×3 structures denoting a $3 \times 3 \times 3$ subpace. The center of this subspace is underlined. If the s.e. is centered at frame i, the first 3×3 structure touches frame $i - 1$, the second structure touches frame i and the last one touches frame $i + 1$. A dot means that the point does not belongs to the s.e., while a bullet means that the point belongs to it.

The s.e. B_6 and B_{26} represents, respectively, the classical 6 and 26-connectivity. The first one is 4-connected in the frame where it is centered and touches the previous and next frames with one point connected to the center of the s.e. along the time axis. The 26-connect s.e. is a cube that touches the frame the s.e. is centered, the previous frame and the next one. The B_5 s.e. is similar to B_6, except that B_5 does not have the point that touches the previous frame. The B_{17} s.e. is similar to B_{26}, except B_{17} does not have any points touching the previous frame: it is a $3 \times 3 \times 2$ pararellepiped s.e..

All of it means that the spatio-temporal gradient and the 3-D watershed computed using the B_6 and B_{26} s.e. consider three frames in their computations: the current frame, the previous and the next ones. When the cited methods applies B_5 and B_{17} to do the spatio-temporal segmentation, just the current and the next frames are considered.

2.2 Band Sequence Extraction

In order to compute the spatio-temporal gradient for color sequences, it is convenient to define an operator that receives a multiband sequence and the desired band and outputs the sequence of the selected band.

Let $\beta : Fun[F,C] \times \{1,2,3\} \rightarrow Fun[F,K]$ be the operator that extracts the band sequence from a multiband sequence, given by,

$$\beta(cs,i)(x) = s_i,$$

where $cs(x) = (s_1,s_2,s_3)$, $\forall cs \in Fun[F,C]$, $\forall x \in F$.

2.3 Spatio-temporal Gradient

Let $gs \in Fun[F,K]$. The operator $\nabla_{B_{3D}} : Fun[F,K] \rightarrow Fun[F,K]$ computes the graylevel 3-D morphological gradient, given by,

$$\nabla_{B_{3D}}(gs)(x) = \bigvee_{y \in B_{3D_x}} gs(y) - \bigwedge_{y \in B_{3D_x}} gs(y).$$

where B_{3D} is a 3-D s.e., $\forall x \in F$. B_{3D_x} is the s.e. B_{3D} translated to the point $x \in F$.

Let $cs \in Fun[F,C]$. The operator $\nabla^c_{B_{3D}} : Fun[F,C] \rightarrow Fun[F,K]$ computes the multiband 3-D morphological gradient, given by,

$$\nabla^c_{B_{3D}}(cs)(x) = \bigvee_{i \in \{1,2,3\}} \nabla_{B_{3D}}(\beta(cs,i))(x),$$

where B_{3D} is a 3-D s.e., $\forall x \in F$.

2.4 Sequence Sampling

Let $\varsigma_i : Fun[F,K] \rightarrow Fun[E,K]$ be the operator that extracts a frame from a gs sequence, given by,

$$\varsigma_i(gs)(x,y) = gs(x,y,i),$$

where $(x,y) \in E$. This function is used to extract the gradient from the i-th frame of the spatio-temporal gradient image deck in order to apply the watershed from markers to it.

3 WATERSHED FROM PROPAGATED MARKERS

The watershed from propagated markers (Flores and Lotufo, 2003) consists, basically, in the following steps:

1. The objects of interest are segmented by the interactive watershed from markers, in the initial frame.
2. The segmentation mask, given by the segmented objects, is broken in pieces closer to the border of the mask. These pieces are regions that form the set of inner markers.
3. In a similar way, the inner markers are computed, the background region is also broken in pieces closer to the border of the mask. The set of outer markers will be formed by these regions.
4. Each marker is propagated to the next frame by motion estimation (B. Lucas and T. Kanade, 1981; B.K.P. Horn and B.G. Schunck, 1981; Gonzalez and Woods, 1992). These new set of inner and outer markers are used to apply the watershed technique to the next frame. Go to the next frame and apply the watershed from markers with the set of computed markers.
5. If necessary, the user interacts with the markers, doing the corrections by adding or moving markers.
6. If the sequence is not fully processed, then go to Step 2.

(In the first proposal of the watershed from propagated markers, the inner markers were computed (Step 2) by taking the contour of erosion of the mask and breaking it in short segments. Similarly, the outer markers were obtained (Step 3) by splitting the contour of erosion of the background region in short segments).

The method proposed above works fine with bad defined contours or strongly textured objects, since the markers are imposed close to the borders of the objects to be segmented. If the quality of segmentation is not approved in some frame, the user can easily move the short-segment marker. The marker propagation is very fast since each segment consists in a few points. Moreover, the contours follow the object deformation, since new markers are created from the segmentation of each frame. The object to be segmented is processed until the end of sequence or until it leaves the scene or be totally occluded. If is partially occluded, the user may intervene to regularize the process.

3.1 Binding of Markers

The *binding of markers* (F. C. Flores and R. A. Lotufo, 2007) is an improvement to the watershed from propagated markers framework. It consists in to compute pairs of markers along the border, and each pair is composed by an internal marker and an external one. Both markers in the pair must be propagated by the same displacement vector, and this vector is computed by the motion estimation of the area *between* the pair of markers. Besides to provide more information to the motion estimation (both markers *and* the area between them), the binding of markers heuristics helps the motion of the pair of markers to follow the motion of the border that crosses the region between them in the previous frame.

3.2 Spatio-temporal Gradient Improvement

The watershed from markers applied to in Step 4 of the framework described in the beginning of this Section uses the markers provided by the binding of markers heuristics. Since the first proposal of the watershed from propagated markers, the watershed operator was always applied directly to the gradient computed from the frame to be segmented at instant i. Let s be the input sequence and $s(i)$ the frame to be segmented. If $s(i) \in Fun[E,K]$ (i.e., a grayscale image), the morphological gradient was computed by the classical way. If $s(i) \in Fun[E,C]$ (i.e., a color image), some metrics were applied to compute the color gradient (F. C. Flores, A. M. Polidório and R. A. Lotufo, 2006; F. C. Flores, A. M. Polidório and R. A. Lotufo, 2004). Anyway, the gradient computation was an intra-frame process, computed by using just the information contained in the frame of interest. It was not exploited any temporal information in the gradient computation.

The spatio-temporal gradient improvement consists in a 3-D morphological processing of the input sequence. Instead to compute the intra-frame gradient in Step 4 each time the watershed is applied to, the spatio-temporal gradient is computed at once, at the beginning of the watershed from propagated markers framework, before Step 1. Let s be an image sequence. The spatio-temporal gradient $tg \in Fun[F,K]$ is given by,

$$tg = \begin{cases} \nabla^{c}_{B_{3D}}(s), & \text{if } s \text{ is a color sequence,} \\ \nabla_{B_{3D}}(s), & \text{otherwise,} \end{cases}$$

where B_{3D} is a 3-D s.e. such as the examples in Section 2.

As stated above, the spatio-temporal gradient tg is a function from F to K, i.e., it is a grayscale sequence. The watershed transform could be applied to tg but, as discussed in the Introduction, it is an expensive process, propagates interframe error and requires an inspection in the whole segmentation sequence every time it is applied to. Even when the sequence was sampled, in previous experiments, with two or three consecutive frames, the interframe error worsened the segmentation result.

The solution is to sample just the i-th frame of the spatio-temporal gradient when it is desired to segment the i-th frame of the input sequence. The sample is an image in $Fun[E,K]$ but contains spatio-temporal information obtained in the spatio-temporal gradient computation. Since it is just a single frame, the interframe error propagation does not occur.

Let $tg \in Fun[F,K]$ be a spatio-temporal gradient. The gradient $g \in Fun[E,K]$ where the watershed from markers will be applied to in Step 4 of the watershed from propagated markers is given by

$$g = \varsigma_i(tg),$$

where i is the index to the i-th frame to be segmented.

4 EXPERIMENTAL RESULTS

Two experiments were done in order to illustrate the gains of productivity and segmentation quality provided by the application of the spatio-temporal gradient to the binding of markers framework. First experiment shows the gains achieved to the first 150 frames of *Foreman* sequence. The second experiment shows the experimental results to the first 150 frames of *Carphone* sequence.

Both experiments apply an benchmark proposed in (F. C. Flores and R. A. Lotufo, 2008) to do a quantitative assessment of interactive object segmentation to image sequences. The benchmark evaluates several measurements such as quality of segmentation and time spent to complete the segmentation task. In that work, several applications of the binding of markers supported by the Lucas-Kanade (B. Lucas and T. Kanade, 1981) motion estimator were tested and compared to. The application that presented the best overall results was the one with parameters $\mathbf{m} = \mathbf{w} = 10$. These parameters and the cited motion estimator were used in all experiments done with *Foreman* and *Carphone* sequences in this paper.

The experiment, for each sequence, consists in to compare several applications of the binding of markers supported by the spatio-temporal gradient to the manual segmentation and to the simple binding of markers application (the one proposed in (F. C. Flores and R. A. Lotufo, 2007)). Table 1 shows the quantitative results for both sequences. Four 3-D s.e. were tested to compute the spatio-temporal gradients: B_5, B_6, B_{17} and B_{26} (see Section 2). When the s.e. used to compute the spatio-temporal gradient were B_5 or B_6, the chosen connectivity for the watershed operator was 4 (the cross s.e.). When the spatio-temporal gradient was computed using B_{17} or B_{26}, the chosen connectivity for the watershed was 8 (the box s.e.). The manual segmentations were used as the groundtruth segmentations. The application of the spatio-temporal gradient is denoted in Table 1 by $\nabla_{B_{3D}}$ and

Table 1: Quantitative assessment of binding of markers improvements. Applications to *Foreman* and *Carphone* sequences (150 frames each sequence).

Method	# Interferences	Time (Secs.)	Time (Mean / Frame)	Segm. Error (Mean / Frame)
FOREMAN				
Manual	3990	12266	81.7733 secs.	-
Binding of Markers	80	1001.6	6.6771 secs.	1.6434 %
∇_{B_5} and $\mathcal{W}_{B_4}$	44	856.2670	5.7084 secs.	1.1340 %
∇_{B_6} and $\mathcal{W}_{B_4}$	46	883.7500	5.8917 secs.	1.2281 %
$\nabla_{B_{17}}$ and $\mathcal{W}_{B_8}$	67	924.4520	6.1630 secs.	1.4288 %
$\nabla_{B_{26}}$ and $\mathcal{W}_{B_8}$	51	869.9540	5.7997 secs.	1.7078 %
CARPHONE				
Method	# Interferences	Time (Secs.)	Time (Mean / Frame)	Segm. Error (Mean / Frame)
Manual	2533	10429	69.5282 secs.	-
Binding of Markers	90	1064.1	7.0962 secs.	0.78 %
∇_{B_5} and $\mathcal{W}_{B_4}$	35	802.2650	5.3484 secs.	0.9697 %
∇_{B_6} and $\mathcal{W}_{B_4}$	30	773.7030	5.1580 secs.	0.9144 %
$\nabla_{B_{17}}$ and $\mathcal{W}_{B_8}$	28	770.0460	5.1336 secs.	1.1171 %
$\nabla_{B_{26}}$ and $\mathcal{W}_{B_8}$	33	777.2950	5.1820 secs.	1.1625 %

the watershed by a connectivity s.e. is denoted by $\mathcal{W}_{B_c}$. In all experiments, an user interference consists in the addition of points or lines segments as markers or in the removal of misplaced markers.

The experiments show that the application of the spatio-temporal gradient provides a decrease in the number of interferences, also providing in some cases a improvement in the segmentation results.

4.1 Foreman Sequence

Several authors use the *Foreman* sequence to demonstrate the performance of their methods, from sequence segmentation techniques to video coding (P. Smith; T. Drummond and R. Cipolla, 2004; P. Salembier *et al*, 1997; F. Moscheni; Sushil Bhattacharjee and Murat Kunt, 1998). Unfortunately, the great majority of such methods is automatic and it is hard to do a fair comparison among these methods using the proposed benchmark since it does not apply to them.

Foreman is a very interesting sequence because it presents many important test situations. The foreman himself, for instance, while he appears in the scene, moves his head in many directions (left, right and forward and backward, what provides a zooming sensation of the foreman face). Foreman head also sometimes rotates, what gives a kind of deformation of the object of interest. Camera is also moving in a smooth but uncontrolled way. If the foreman is the object of interest, note that he is composed by several objects that need to be segmented and tracked: the helmet, his face and jacket. More, the sequence presents several regions of low contrast such as the foreman shoulder, his ears and the region where helmet meets the white concrete background. *Foreman* sequence is not a trivial task to segment appropriately.

Table 1 - Part One shows the evaluation of six experiments: the ground-truth provided by manual segmentation, the simple binding of markers and four applications of the binding of markers supported by spatio-temporal gradients. Except for the third spatio-temporal case ($\nabla_{B_{17}}$ and $\mathcal{W}_{B_8}$), all spatio-temporal cases required about a half of user effort to complete the task, compared to the simple binding of markers framework. And, except for the forth spatio-temporal case ($\nabla_{B_{26}}$ and $\mathcal{W}_{B_8}$), all spatio-temporal cases provided a better segmentation result, again compared to the simple binding of markers approach. Note that all spatio-temporal approaches were faster than the simple binding of markers to segment the foreman.

Figures 1 and 2 show some graphical information about *Foreman* sequence and the application of the binding of markers in two versions: the simple one and the improved by the spatio-temporal gradient - this one, using ∇_{B_5} and $\mathcal{W}_{B_4}$ as s.e.. Figure 1 (a) shows the amount of motion in *Foreman* sequence (computed by the symmetrical difference between consecutive frames) and Fig. 1 (b) shows the number of user interferences for the two examples: solid magenta plotting shows the number of interferences required in the simple binding of markers application and the dot-dashed black plotting shows the number of interferences for the spatio-temporal case.

Figure 2 (a) shows the plotting of the time needed to segment each frame for the two example cases (solid magenta plotting for the simple case, dot-

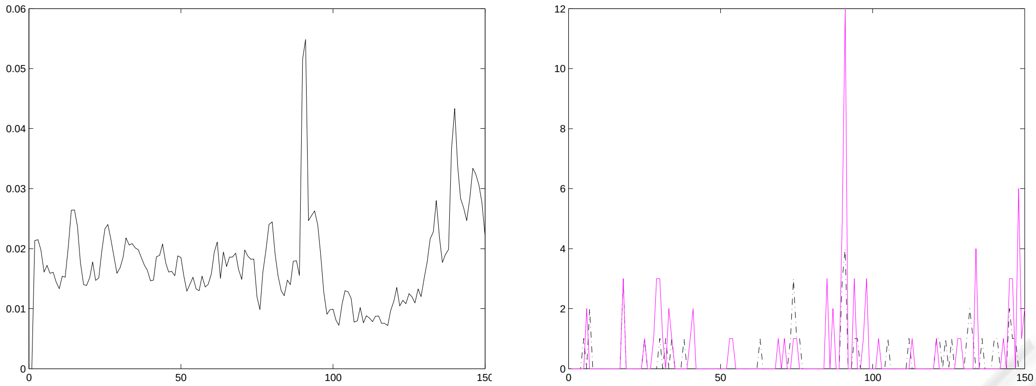

(a) (b)

Figure 1: Quantitative evaluation for *Foreman* sequence. (a) Motion information from *Foreman* sequence. (b) Number of interferences for each frame.

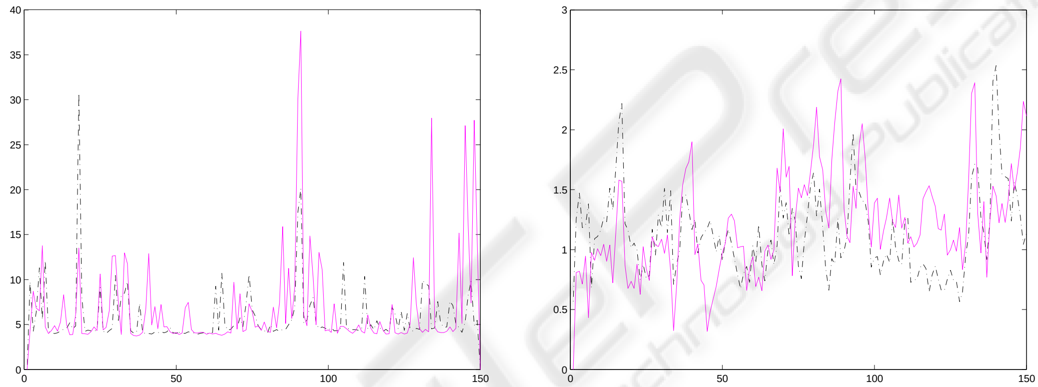

(a) (b)

Figure 2: Quantitative evaluation for *Foreman* sequence. (a) Time spent in each frame (secs.). (b) Segmentation error (Percentile. Compared to the ground-truth).

dashed black plotting for the spatio-temporal one). Note that the amount of efforts and time shown, respectively in Fig. 1 (b) and Fig. 2 (a) are consistent with the plotting with the image motion in Fig. 1 (a). Finally, Fig. 2 (b) shows the plotting of the segmentation error for each frame. In overall, the spatio-temporal case had a lower error in most of the cases.

Figure 3 shows the segmentation of *Foreman* sequence using ∇_{B_5} and $\mathcal{W}_{B_4}$. It is shown the segmentation of the first 150 frames of the sequence.

4.2 Carphone Sequence

The segmentation of the man in *Carphone* sequence is also a difficult task. *Carphone* is also a very used sequence in the demonstration of image sequence processing techniques. The goal in this experiment was to segment the passenger from the remain of the scene. The passenger moves his body in several directions through the sequence, rotating slightly the body and approaching the face to the camera in a given instant. There are moments when the separation of the left shoulder and the ear regions from the background is difficult. More, the is also movement outside the car window. The passenger is composed by several objects: his head, which has difficult regions to segment and his hair, and the body, that is a easiest part to segment. However, the region where the left shoulder meets the window has a low constrast and a strong source of segmentation error.

Table 1 - Part Two shows the segmentation evaluation of six experiments, the same applied to the *Foreman* sequence. Note that all mean segmentation errors were close to 1%. The common binding of markers provided the best mean segmentation result, but not too much better than the ones provided by the spatio-temporal supported applications. Note, however, that the number of interferences decreased drastically in the spatio-temporal gradient approaches: simple binding of markers approach required 90 interferences. The spatio-temporal approaches required a third less effort to complete the task: they re-

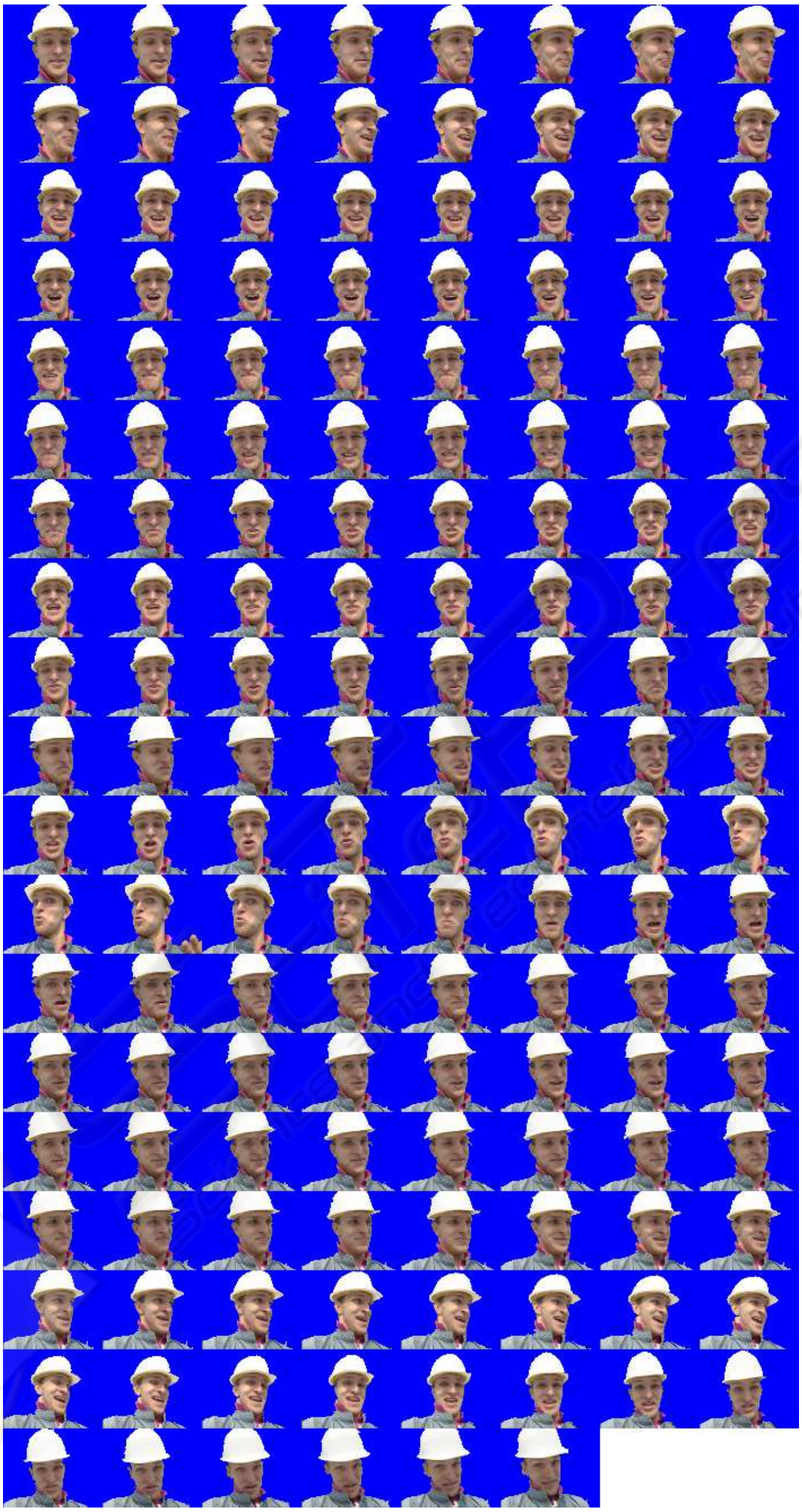

Figure 3: Segmentation of *Foreman* sequence (frames 1 to 150). Using ∇_{B_5} and $\mathcal{W}_{B_4}$.

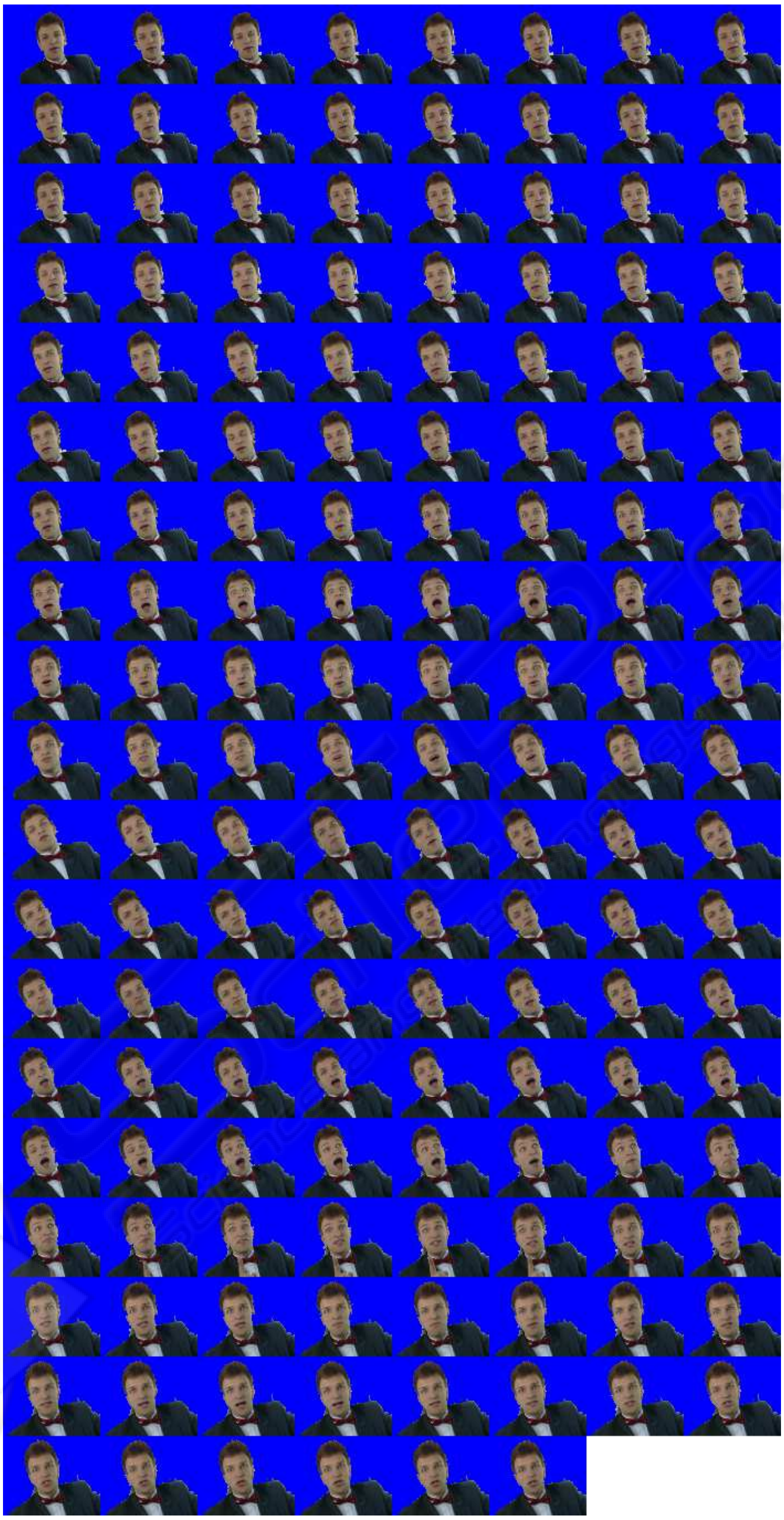

Figure 4: Segmentation of *Carphone* sequence (frames 1 to 150). Using $\nabla_{B_{17}}$ and w_{B_8}.

quired about 30 interferences, a very good improvement compared to the simple binding of markers approach.

Figure 4 shows the segmentation of *Carphone* sequence using $\nabla_{B_{17}}$ and $\mathcal{W}_{B_8}$. It is shown the segmentation of the first 150 frames of the sequence.

5 CONCLUSIONS

This paper introduces an improvement to the watershed from propagated markers: the combination of binding of markers heuristics with the spatio-temporal gradient. The main idea consists in, for a given frame, to apply the watershed from markers to an image extracted from an 3-D gradient sequence, computed by a morphological processing using a 3-D s.e.. The applied markers were computed by the binding of markers heuristics.

Experiments were done in order to assess the impact of the addition of the spatio-temporal gradient to the watershed from propagated markers framework and this addition provided a increasing in the segmentation performance. The decrease in the number of interferences was significant and the quality of segmentation was improved even with a lower number of user interferences. Time segmentation decreased as well.

Future works include the study of the spatio-temporal gradient properties in order to improve the segmentation results provided by the watershed from propagated markers technique.

REFERENCES

B. Lucas and T. Kanade (1981). An interative image registration technique with an application to stereo system. In *Proceedings of DARPA Image Understanding Workshop*, pages 121–130.

Beucher, S. and Meyer, F. (1992). *Mathematical Morphology in Image Processing*, chapter 12. The Morphological Approach to Segmentation: The Watershed Transformation, pages 433–481. Marcel Dekker.

B.K.P. Horn and B.G. Schunck (1981). Determining Optical Flow. *Artificial Intelligence*, 17:185–204.

F. C. Flores, A. M. Polidório and R. A. Lotufo (2004). Color Image Gradients for Morphological Segmentation: The Weighted Gradient Improved by Automatic Imposition of Weights. In *SIBGRAPI*, pages 146–153, Curitiba, Brazil.

F. C. Flores, A. M. Polidório and R. A. Lotufo (2006). The Weighted Gradient: A Color Image Gradient Applied to Morphological Segmentation. *Journal of the Brazilian Computer Society*, 11(3):53–63.

F. C. Flores and R. A. Lotufo (2007). Watershed from Propagated Markers Improved by a Marker Binding Heuristic. In G.J.F. Banon, J. B. and Braga-Neto, U., editors, *Mathematical Morphology and its Applications to Image and Signal Processing*, Proc. ISMM'07, pages 313–323. MCT/INPE.

F. C. Flores and R. A. Lotufo (2008). Benchmark for Quantitative Evaluation of Assisted Object Segmentation Methods to Image Sequences. In *IEEE Proceedings of SIBGRAPI'2008*, pages 95–102, Campo Grande, Brazil.

F. C. Flores and R. A. Lotufo (2009). Watershed from Propagated Markers: An Interactive Method to Morphological Object Segmentation in Image Sequences. *To Appear on Image and Vision Computing*.

F. Moscheni; Sushil Bhattacharjee and Murat Kunt (1998). Spatiotemporal Segmentation Based on Region Merging. *IEEE Transactions on Pattern Analysis and Machine Intelligence*, 20(9):897–915.

Flores, F. C. and Lotufo, R. A. (2003). Object Segmentation in Image Sequences by Watershed from Markers: A Generic Approach. In *IEEE Proceedings of SIBGRAPI'2003*, pages 347–352, Sao Carlos, Brazil.

Gonzalez, R. C. and Woods, R. E. (1992). *Digital Image Processing*. Addison-Wesley Publishing Company.

J. L. Barron; D. J. Fleet and S. S. Beauchemin (1994). Performance of Optical Flow Techniques. *International Journal of Computer Vision*, 12(1):43–77.

P. Salembier *et al* (1997). Segmentation-Based Video Coding System Allowing the Manipulation of Objects. *IEEE Transactions on Circuits and Systems for Video Technology*, 7(1):60–74.

P. Smith; T. Drummond and R. Cipolla (2004). Layered Motion Segmentation and Depth Ordering by Tracking Edges. *IEEE Transactions on Pattern Analysis and Machine Intelligence*, 26(4):479–494.

S. S. Beauchemin and J. L. Barron (1995). The Computation of Optical Flow. *ACM Computing Surveys*, 27(3):433–467.

Soille, P. and Vincent, L. (1990). Determining Watersheds in Digital Pictures via Flooding Simulations. In *Visual Communications and Image Processing*, pages 240–250. SPIE. volume 1360.